

Numerical investigation of electrostrictive forces in submicron phoxonic waveguide

Jean-Charles Beugnot and Vincent Laude

Institut FEMTO-ST, Université de Franche-Comté, CNRS UMR 6174, 25044 Besançon cedex, France

ABSTRACT

We demonstrate that the acoustic phonons involved in stimulated Brillouin scattering (both forward and backward) in phoxonic waveguide can be completely described by using electrostrictive forces. Numerical calculation for bridge waveguide in silicon and silica illustrate the model.

Keywords: Brillouin scattering, electrostriction, phoxonic waveguide

1. INTRODUCTION

Nanostructured photonics (x=t,n) crystal waveguides have been investigated recently numerically and experimentally in view of obtaining simultaneous confinement of elastic and optical waves.^{1,2} Their interaction can be controlled by optical forces such as radiation pressure,³ which is predicted to scale to large values in nanoscale waveguides.⁴ Furthermore, Brillouin scattering is a nonlinear process where two photons generate a co-propagating acoustic phonon through electrostriction.⁵ This phenomenon is broadly documented for silica optical fibers, in both theory and experiment.⁶ Nevertheless, a general model including electrostriction forces is still needed to understand the optoacoustic interaction and to design ultra efficient optoacoustic devices. In this paper, we perform numerical calculations of electrostriction forces for the Brillouin scattering phenomenon in different phoxonic submicron waveguides. After calculation of the optical guided modes of the waveguide by using the finite element method, the electrostriction-driven acoustic equation is solved for the displacement of the elastic wave by setting the acoustic wave vector and scanning the detuning frequency between the two optical waves. With this model, and according to the phase matching condition, we fully characterize Brillouin properties of phoxonic waveguides, including backward and forward Brillouin spectra, without the need to resort to a full band structure computation.⁷

2. ELECTROSTRICTION FORCE

Brillouin scattering process is a third-order parametric process where a pump photon (k_1, ω_1) produces a downshifted Stokes photon (k_2, ω_2) and an acoustic phonon (K, Ω). The electrostriction of acoustic wave is obtained from the interaction of two incident photons with frequency detuning Ω . The incident optical field is

$$E_k(r, z) = E_k^1(r, z)e^{i(\omega_1 t - k_1 z)} + E_k^2(r, z)e^{i(\omega_2 t - k_2 z)}, \quad (1)$$

with $k_1 = k(\omega_1)$ and $k_2 = k(\omega_2)$ satisfying a dispersion relation for guided waves, and $\Omega = \omega_1 - \omega_2$. It is assumed that the acoustic frequency is small as compared to optical frequencies. The only source term at frequency Ω is proportional to $\exp(i(\Omega t - Kz))$ with $K = k_1 - k_2$. If the two optical waves are co-propagating, this is a Guided Acoustic Wave Brillouin Scattering⁸ (GAWBS) case with $K \approx 0$ and if they are contra-propagative, this is the Stimulated Brillouin backscattering⁹ (SBS) with $K = K_1$.

From band structure computation, conventional SBS treatments in optical fiber determine the Brillouin gain spectrum from the elasto-optic overlap integral^{10,11} but the generation of elastic waves by optical waves is neglected. In our model, the acoustic waves generated by Brillouin scattering are obtained by solving the acoustic wave equation subject to the optical forces that arise from the distribution of light within the waveguide cross-section as a result of electrostriction at the detuning frequency.¹²

Further author information: (Send correspondence to jc.beugnot@femto-st.fr)

Table 1. Silica and silicon parameter using for electrostriction calculation.

Parameter	$n_{@1.55\mu\text{m}}$	ρ (kg/m ³)	p_{11}	p_{12}	p_{44}	c_{11} (Pa)	c_{12} (Pa)	c_{44} (Pa)	Qf (Hz)
Si	3.47	2331	0.10	0.01	0.051	166.10 ⁹	64.10 ⁹	79.10 ⁹	5.10 ¹³
SiO ₂	1.44	2203	0.12	0.27	-0.073	78.10 ⁹	16.10 ⁹	31.10 ⁹	5.10 ¹²

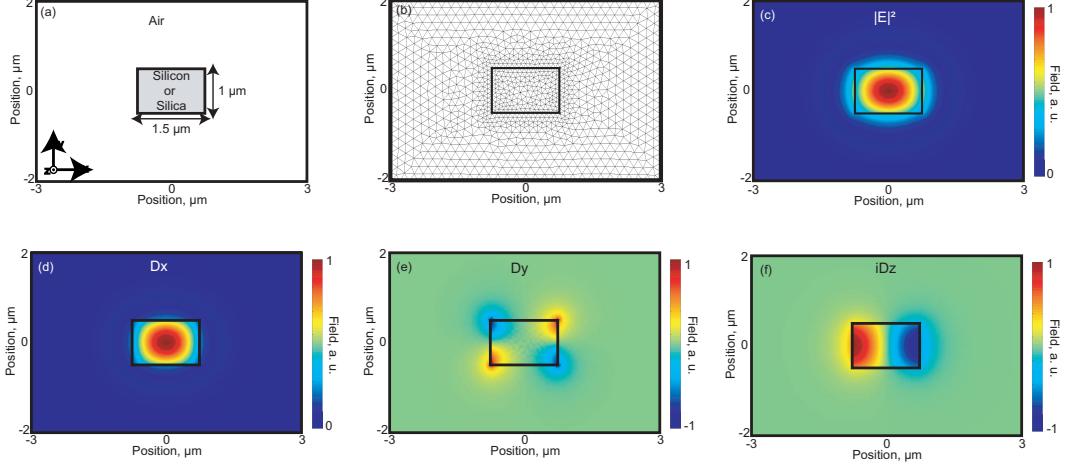


Figure 1. (a,b) Cross section and finite-element mesh of a bridge waveguide with lateral dimensions equal to $1.5\mu\text{m} \times 1\mu\text{m}$. (c) Normalized total electric field, (d) Dx , (e) Dy and (f) iDz components of the fundamental TE-like mode for $\lambda = 1550\text{nm}$.

The variational problem is solved for the displacements u_i , ($i = x, y, z$) by setting K to a given value and scanning the detuning frequency Ω . We further calculate the kinetic energy of the elastic resonance (i.e. Brillouin gain spectrum) as defined by :

$$E_C(\Omega) = \frac{1}{2}\rho\Omega^2(u_x^2 + u_y^2 + u_z^2), \quad (2)$$

with ρ the material density. We consider a bridge waveguide with lateral dimensions equal to $1\mu\text{m}$ by $1.5\mu\text{m}$, as depicted in Fig. 1(a). The solid core, made of silicon (Si) or silica (SiO_2), is surrounded by air ($n=1$). With these dimensions, the effects of radiation pressure are in principle negligible.¹³ The different material constants used in the calculations are presented in Tab. 1. Here, p_{ij} and c_{ij} are the photoelastic-tensor component and elastic constant represented in contracted notation, respectively.¹⁴

3. NUMERICAL MODELLING

We first compute the optical guided waves using a 2D FEM model. Fig. 1(c-f) display different components of the fundamental guided optical mode in the silica bridge for $\lambda = 1550\text{nm}$. To simulate the real Brillouin interaction, elastic losses are incorporated in the electrostriction model by considering a complex elastic tensor $c_{ijkl} + i\Omega\eta_{ijkl}$ where η_{ijkl} is a viscosity tensor.¹⁵ This loss model is compatible with the usual assumption that the Qf product is constant for a given material. The symmetry of the viscosity tensor is the same as that of the elastic tensor. The viscosity constants are hardly available in the literature for silicon and silica. For silicon wafers, we estimated $Qf = 5.10^{13}\text{Hz}$ from independent experiments performed with bulk acoustic wave resonators. From measurements of the SBS linewidth in standard optical silica fiber, we estimated $Qf = 5.10^{12}\text{Hz}$. So far, we have assumed that the loss factor for shear and longitudinal elastic waves is identical, but the model can consider a fully anisotropic viscosity tensor. The outer boundaries of the analysis region are treated as free boundaries. The analysis region is taken to be sufficiently large so that the effect of these virtual boundaries can be neglected in practice. The kinetic energy of resonant elastic waves (i.e., the Brillouin gain spectrum) for the GAWBS and

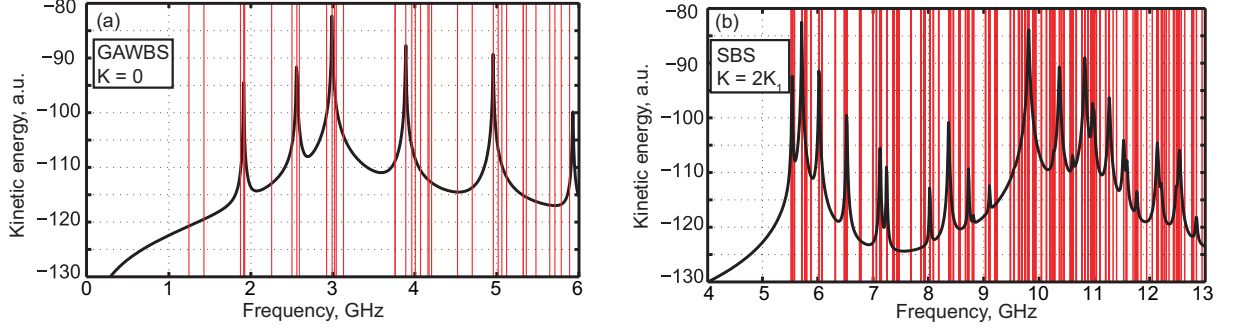


Figure 2. Computed elastic energy as a function of frequency detuning Ω for the silica bridge waveguide in (a) the GAWBS and (b) the SBS configurations. The red vertical lines mark the eigenfrequencies of the purely-acoustic problem.

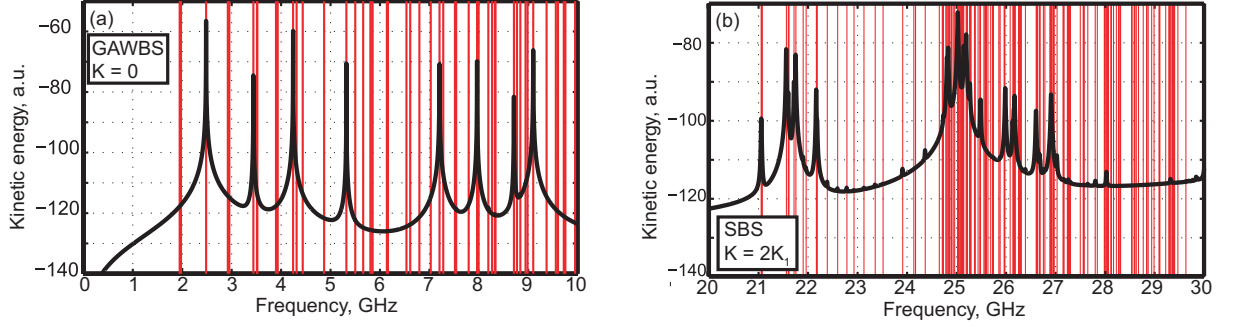


Figure 3. Computed elastic energy as a function of frequency detuning Ω for the silicon bridge waveguide in (a) the GAWBS and (b) the SBS configurations. The red vertical lines mark the eigenfrequencies of the acoustic problem.

the SBS processes in silica and silicon bridge are presented in Fig. 2 and Fig. 3, respectively. We superimpose on the Brillouin gain spectrum the eigenfrequencies solution obtain without the optical force term, i.e., from the homogeneous problem. The frequencies of elastic resonances calculated by our electrostriction model clearly correspond to eigenfrequency solutions, but with added information on the detailed spectral distribution of the Brillouin gain. It should be noted that our model is valid for all types of phoxonic waveguides, optical fibers, and can be useful to explain the broadening of Brillouin spectrum that is experimentally observed.^{16,17}

It comes as a very good surprise that the case of silicon seems to be favourable over the case of silica (Fig. 3). Indeed, Brillouin scattering in silica optical fibers is broadly documented and not too difficult to observe. The literature generally attributes this fact to the good $p_{12} = 0.27$ value that is highly favorable for longitudinal acoustic waves. In the case of silicon, $p_{12} = -0.01$ is very small. However, $p_{11} = -0.1$ favors shear acoustic waves in silicon. Combined with the much higher relative permittivity and the lower loss of silicon, this fact explains the computation results. We can further obtain the modal distribution of acoustic phonons at any frequency for the silica bridge waveguide. The strongest scattering peak in Fig. 2a appears at 2.99 GHz. This frequency is directly related to the dimensions of the waveguide. This elastic resonance contains only the contribution of the transverse deformation $u_T = (u_x^2 + u_y^2)^{0.5}$ represented in Fig. 4.

The calculated backscattering Brillouin gain spectrum in the silica bridge waveguide shows two important elastic resonances at 9.81 GHz and 5.71 GHz. The real part of displacement distribution and the corresponding kinetic energy are presented in Fig. 5(a,b). As can be seen, the kinetic energy of the elastic mode at 9.81 GHz is stronger over the core region where the optical mode distribution is at a maximum. This configuration is radically different from the GAWBS case, where the deformation is stronger in the bridge cladding than in the core (Fig. 4).

The frequency of the elastic resonance at 9.81 GHz is directly related to the phase matching condition ($K = 2K_1$). In this case, the longitudinal displacement u_L dominates the total deformation, as seen in Fig. 5(a). As a comparison, the total displacement of the elastic resonance at the frequency of 5.71 GHz is dominated by

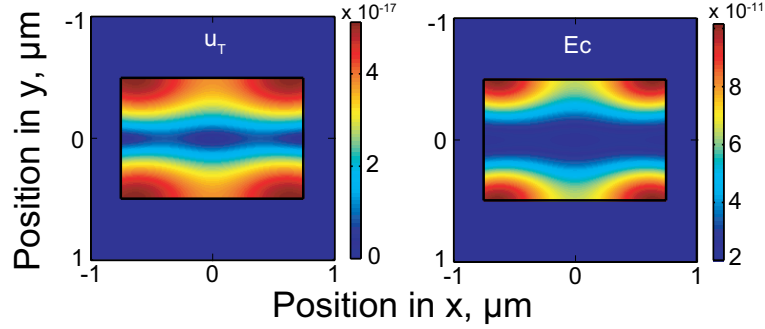


Figure 4. Spatial distribution of the transverse deformation (u_T) and the kinetic energy (E_C) of the elastic mode at 2.99 GHz in the silica bridge waveguide for the GAWBS configuration.

the transverse components as can be seen in Fig. 5(d-f). The transverse component was verified to be 0.76 of the longitudinal component. This elastic resonance originates from Rayleigh surface waves overlapping with the guided optical mode.¹⁸ This wave does not exist in bulk glass and standard silica optical fiber because the photonic waveguide defined by the germanium doped core region is surrounded by a large silica cladding.¹⁹ Fig. 6(a,b) show the Brillouin gain spectrum for the GAWBS and SBS configurations respectively, as the waveguide scale factor varies between 0.8 to 2. The appearance of multiple peaks in the 10 GHz region for small dimensions is clearly apparent. For the SBS configuration, we demonstrate the optical excitation of different phonons in the dispersion band diagram as the dimensions are varied. This result is radically different from the GAWBS configuration where the frequency resonance decreases linearly with the core dimension. In contrast, this result is very similar to photonic crystal fiber where the small core exhibits the generation of high frequency resonances directly related to the core dimension.^{20,21} For large scale factors (up to 5), the Brillouin backscattering gain spectrum becomes a simple Lorentzian, the frequency resonance of which perfectly respects the phase matching condition.⁵

4. CONCLUSION

We have presented a Brillouin scattering model where electrostriction forces are included. Whereby, we have identified the phonons that are excited by photons in phoxonic waveguides in forward and backward Brillouin configuration. Based on the finite element method, the spatial distribution of the elastic wave properties strengthens the understanding of this type of optoacoustic interaction. We have demonstrated that silicon waveguides seem to favor Brillouin scattering over silica waveguides. The combination of large relative permittivity and high simultaneous confinement of photons and phonons explains the computation result. The calculation of electrostriction forces in phoxonic waveguides involves the simultaneous control of photons and acoustic phonons, thereby potentially improving the performance and overcoming some limits of current integrated devices.

ACKNOWLEDGMENTS

This work was supported by the European program INTERREG IV (CD-FOM) and the European Community's Seventh Framework program (FP7/2007-2013) under grant agreement number 233883 (TAILPHOX).

REFERENCES

- [1] Alegre, T. P. M., Safavi-Naeini, A., Winger, M., and Painter, O., "Quasi-two-dimensional optomechanical crystals with a complete phononic bandgap," *Optics Express* **19**(6), 5658–5669 (2011).
- [2] Laude, V., Beugnot, J.-C., Benchabane, S., Pennec, Y., Djafari-Rouhani, B., Papanikolaou, N., Escalante, J. M., and Martinez, A., "Simultaneous guidance of slow photons and slow acoustic phonons in silicon phoxonic crystal slabs," *Optics Express* **19**(10), 9690–9698 (2011).
- [3] Eichenfield, M., Chan, J., Camacho, R. M., Vahala, K. J., and Painter, O., "Optomechanical crystals," *Nature* **462**(7269), 78–82 (2009).

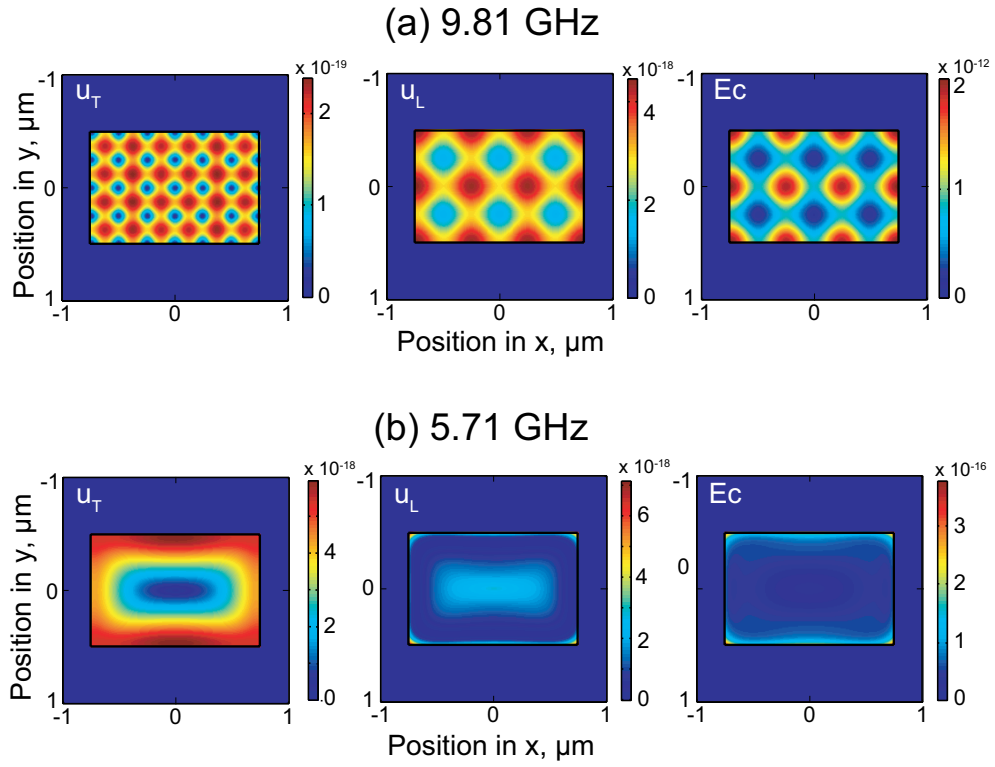


Figure 5. Spatial distribution of elastic mode for SBS configuration in silica bridge waveguide. Top row, 9.81 GHz; bottom row, 5.71 GHz; from left to right u_T, u_L, E_C .

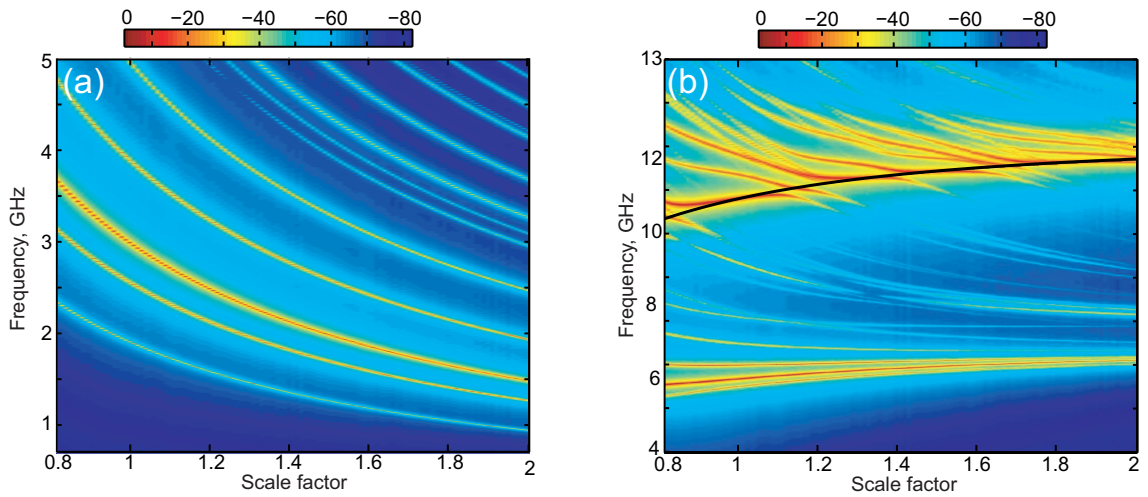


Figure 6. (a) GAWBS and (b) SBS spectrum as a function of scale factor in silica bridge. For scale factor equal to 1, the GAWBS and SBS spectrum is presented in fig 2(a,b) respectively. For SBS configuration, the black line represent the phase matching condition ($K = 2K_1$).

- [4] Kippenberg, T. J. and Vahala, K. J., “Cavity optomechanics: Back-action at the mesoscale,” *Science* **321**(5893), 1172–1176 (2008).
- [5] Boyd, R. W., [*NonLinear Optics*], San Diego (1992).
- [6] Kobayakov, A., Sauer, M., and Chowdhury, D., “Stimulated brillouin scattering in optical fibers,” *Adv. Opt. Photon.* **2**(1), 1–59 (2010).
- [7] Laude, V., Khelif, A., Benchabane, S., Wilm, M., Sylvestre, T., Kibler, B., Mussot, A., Dudley, J. M., and Maillotte, H., “Phononic band-gap guidance of acoustic modes in photonic crystal fibers,” *Phys. Rev. B* **71**, 045107 (2005).
- [8] Shelby, R., Levenson, M., and Bayer, P., “Guided acoustic-wave brillouin scattering,” *Phys. Rev. B* **31**, 5244–5252 (1985).
- [9] Chiao, R. Y. and Townes, C., “Stimulated brillouin scattering and coherent generation of intense hypersonic waves,” *Phys. Rev. Lett.* **12**(21), 592–595 (1964).
- [10] McCurdy, A. H., “Modeling of stimulated brillouin scattering in optical fibers with arbitrary radial index profile,” *J. of Light. Tech.* **23**(11), 3509–3516 (2005).
- [11] Dasgupta, S., Poletti, F., Liu, S., Petropoulos, P., Richardson, D. J., Grüner-Nielsen, L., and Herstrøm, S., “Modeling brillouin gain spectrum of solid and microstructured optical fibers using a finite element method,” *J. Lightwave Technol.* **29**(1), 22–30 (2011).
- [12] Carlson, C. G., Ross, R. B., Schafer, J. M., Spring, J. B., and Ward, B. G., “Full vectorial analysis of brillouin gain in random acoustically microstructured photonic crystal fibers,” *Phys. Rev. B* **83**, 235110 (2011).
- [13] Rakich, P. T., Reinke, C., Camacho, R., Davids, P., and Wang, Z., “Giant enhancement of stimulated brillouin scattering in the subwavelength limit,” *Phys. Rev. X* **2**, 011008 (2012).
- [14] Royer, D. and Dieulesaint, E., [*Ondes elastiques dans les solides Tome 2, Génération, interaction acousto-optique, applications*], Masson (1996).
- [15] Moiseyenko, R. P. and Laude, V., “Material loss influence on the complex band structure and group velocity in phononic crystals,” *Phys. Rev. B* **83**, 064301 (2011).
- [16] Beugnot, J.-C., Sylvestre, T., Alasia, D., Maillotte, H., Laude, V., Monteville, A., Provino, L., Traynor, N., Foalet, S. M., and Thévenaz, L., “Complete experimental characterization of stimulated brillouin scattering in photonic crystal fiber,” *Optics Express* **15**(23), 15517–15522 (2007).
- [17] Zhang, W., Wang, Y., Pi, Y., Huang, Y., and Peng, J., “Influences of pump wavelength and environment temperature on the dual-peaked brillouin property of a small-core microstructure fiber,” *Opt. Lett.* **32**(16), 2303–2305 (2007).
- [18] Thurston, R. N., “Elastic waves in rods and clad rods,” *J. Acoust. Soc. Am* **64**, 1–37 (1978).
- [19] Dainese, P., Russell, P. S. J., Joly, N., Knight, J. C., Wiederhecker, G. S., Fragnito, H. L., Laude, V., and Khelif, A., “Stimulated brillouin scattering from multi-ghz-guided acoustic phonons in nanostructured photonic crystal fibres,” *Nature Physics* **2**(6), 388–392 (2006).
- [20] Beugnot, J.-C., Sylvestre, T., Maillotte, H., Mélin, G., and Laude, V., “Guided acoustic wave brillouin scattering in photonic crystal fibers,” *Optics Letters* **32**(1), 17–19 (2007).
- [21] Kang, M. S., Nazarkin, A., Brenn, A., and Russell, P. S. J., “Tightly trapped acoustic phonons in photonic crystal fibres as highly nonlinear artificial raman oscillators,” *Nature Physics* **5**(4), 276–280 (2009).